Supporting Information

Native Cellulose Microfiber-Based Hybrid Piezoelectric Generator for Mechanical Energy Harvesting Utility

Md. Mehebub Alam and Dipankar Mandal*

Organic Nano-Piezoelectric Device Laboratory, Department of Physics, Jadavpur University, Kolkata 700032, India.

Corresponding author. Tel.: +91 33 2414 6666x2880; Fax: +91 33 2413 8917; E-mail: dipankar@phys.jdvu.ac.in

HPG fabrication. Schematic representation of the fabrication process of the flexible hybrid piezoelectric generator (HPG) is shown in Figure S1. The preparation is described as follows: firstly, cellulose microfiber with MWCNTs is dispersed in PDMS by mechanical agitation on the basis of a mass ratio of cellulose-MWCNTs-PDMS =5: 0.5: 100 as shown in Figure S1a-b. Then mixed solution was poured into petridish like Al-foil mold (Figure S1c). After removal of the bubbles from the solution with the help of a vacuum pump, it was dried at 80^{o} C for 30 m to convert it from solution to a round shaped composite film.

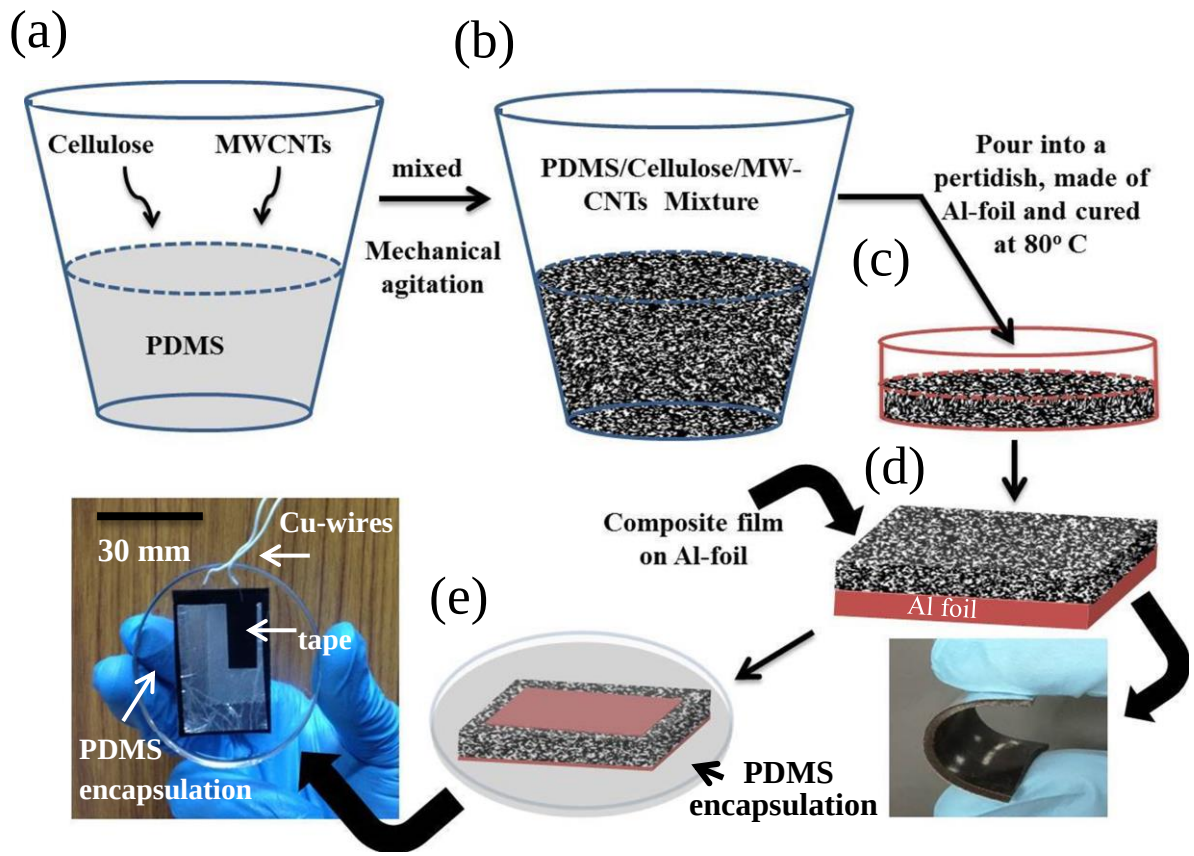

Figure S1. The schematic of HPG fabrication process. (a)- (b) cellulose and MWCNTs are dispersed in PDMS by mechanical agitation in the mass ratio of 5:0.5:100. (c) PDMS-cellulose-MWCNTs mixture was poured into an Al-foil mold petridish and subsequently dried to get a composite film. (d) The composites film, after cutting into a rectangular shape (including the Al-foil at the bottom). The real image of the composite film including the Al-foil underneath is shown at bending state, demonstrating its flexibility. (e) Another Al-foil (33×25 mm^2) is attached to the top surface to serve as an electrode and the entire electrode-composite-electrode structure is covered with a thin pure PDMS layer to protect from direct hitting. The digital photograph of the HPG is also shown.

Flexible composite film attached with Al-foil (act as a bottom electrode) then cut into a rectangular shape of 40 mm of length, 28 mm of width and 2 mm of thickness as shown in the upper image of Figure S1d. The real image of the composite film on the Al-foil, demonstrating its flexibility, is also illustrated from lower image of Figure S1d. Another Al-foil (33×25 mm^2) is physically attached to the upper surface that served as a top electrode. Cu wires were then soldered with Al-electrodes and covered with conducting carbon tape. This sandwich like hybrid piezoelectric generator (HPG) finally encapsulated by pure PDMS layer to protect the HPG from direct hitting (Figure S1e, right side). The digital photograph of the fabricated HPG in the final form is depicted in Figure S1e (left side).

Table S1: Vibrational band assignments of cellulose I revealed from FT-IR spectra, shown in inset of Figure S2. [S1-S4]

Wavenumber (cm^{-1})	**Band Assignment**
897	COC asymmetric stretching
1031	CO at C-6 stretching
1055	CO stretching vibrations
1110	Asymmetric vibration of glucose ring
1161	COC asymmetric vibration
1204	COH in-plane at C-6 bending
1281	CH and OH vibration
1315	COH and HCC vibration
1335	OH and CH_2 vibration
1370	COH and HCC vibration of cellulose and hemicelluloses
1428	CH_2 vibration; HCH and OCH in plane banding; intermolecular hydrogen bond bending
2900	CH and CH_2 vibration presence in aliphatic methylene groups
3340	Stretching vibrations of CH and OH groups

Text S1. Pressure calculation. [S5, S6]

We can calculate the input pressure on the HPG from the following equations,

$$m.g.h = \frac{1}{2}mv^2 \qquad (1)$$

$$(F - m.g).\Delta t = m.v \qquad (2)$$

$$\sigma = \frac{F}{S} \qquad (3)$$

Here, m=2.16 kg is measured by using a laboratory balance, g = 9.8 N/kg, h = 0.05 m, Δt = 0.182 sec is the estimated average time variation between the two consecutive voltage peaks and S= 825 mm^2 is the effective electrode area of the HPG,

Therefore, input force, F~ 33 N and applied stress, $\sigma \sim 40$ kPa.

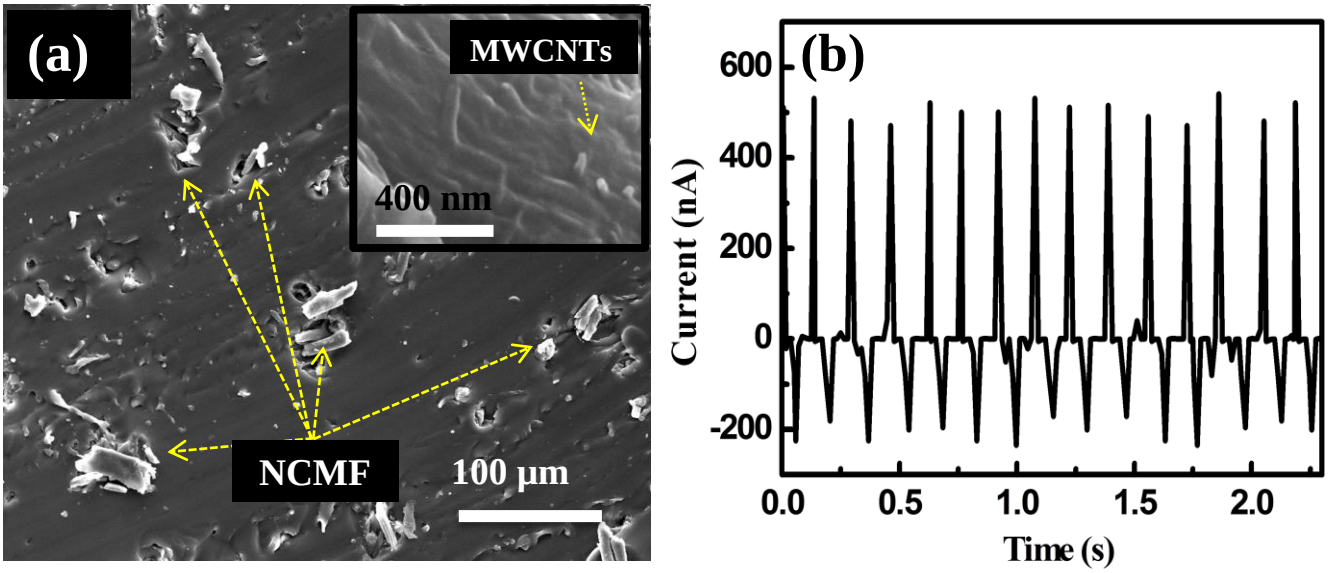

Figure S2. (a) The FE-SEM image of the PDMS-cellulose-MWCNTs composite film. The inset shows the MWCNTs in the composite film (b) Short circuit current from the HPG under repeating human hand punching of the stress amplitude of 40 kPa.

Text S2. Power Calculation.

Power (P) =VI (4)

= 15 μW

$$\text{Power density} = \frac{Power}{Active\ area \times Thickness} = 9.09\ \mu W/cm^3$$

Here, V= 30 V, I=500 nA, active area= 33×25 mm^2, thickness= 2 mm.

Table S2: Comparison of the HPG performance with other reported data.

Piezoelectric components	Poling voltage and duration	Sources/input pressure or force	Voltage (V)	Current (I)	Power density
Cellulose-ZnO [S7]	Not found	Ultrasonic bath/Not found	80 mV	1.25 μA	50 nW/cm^2
ZnO NWs/ paper[S8]	Not found	Not found /Not found	17 mV	400-520 pA	5x10^{-3} μW/cm^2
ZnO NWs/PVDF[S9]	100 kV/mm	Linear motor/Not found	0.2 V	10 nA/cm^2	2 μW/cm^3
$BaTiO_3$ NPs[S10]	100 kV/cm; 20 h	Bending stage/ 57 kPa	3.2V	350 nA	0.26 μW/cm^3
$ZnSnO_3$[S6]	Not Found	Human finger press/ 12kPa	40 V	0.4 μA	10.8 μW/cm^3
$KNbO_3$ Nanorod[S11]	150 kV; 1h	Linear motor/0.38% strain and 15.2% s^{-1} strain rate	3.2 V	67.5 nA	11.9 μW/cm^3
$KNbO_3$ nanowires [S12]	5.0 kV/mm; 1 h	Bending tester/ a strain and strain rate of 2.1% and 2.2% s^{-1}	10.5 V	1.3 μA	42 μW/cm^3
$BaTiO_3$ nanotubes [S13]	80 kV/cm; 12 h	Linear motor/ 1 MPa	5.5 V	350 nA	64 μW/cm^3
KNN-LTS [S14]	2 KV/mm; 24 h	Mechanical tapping/ 933 kPa	53 V	15 μA	115 μW/cm^3
NCMF (present work)	**Not Poled**	**Human hand punching/ 40kPa**	**30 V**	**500 nA**	**9 μW/cm^3**

Mechanism of high output parformance of the HPG:

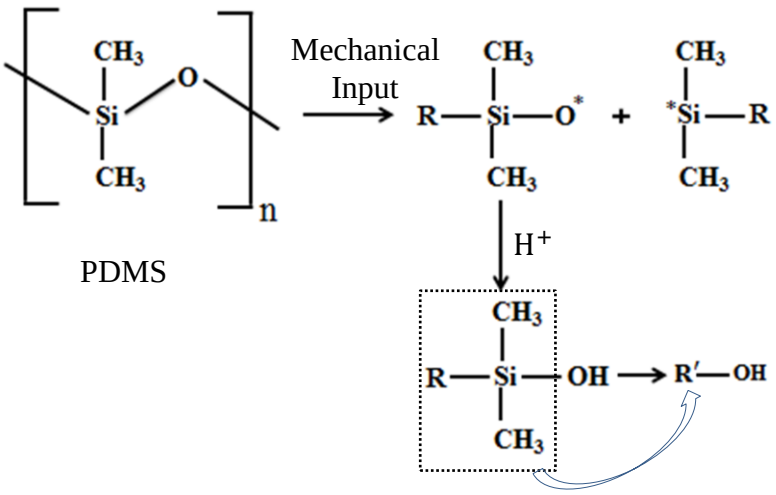

Figure S3. Schematic that illustrates the homolytic (leading to radical) chain breaking of PDMS upon mechanical input.[S15] Reproduced with permission from reference S15. Copyright 2013 Royal Society of Chemistry.

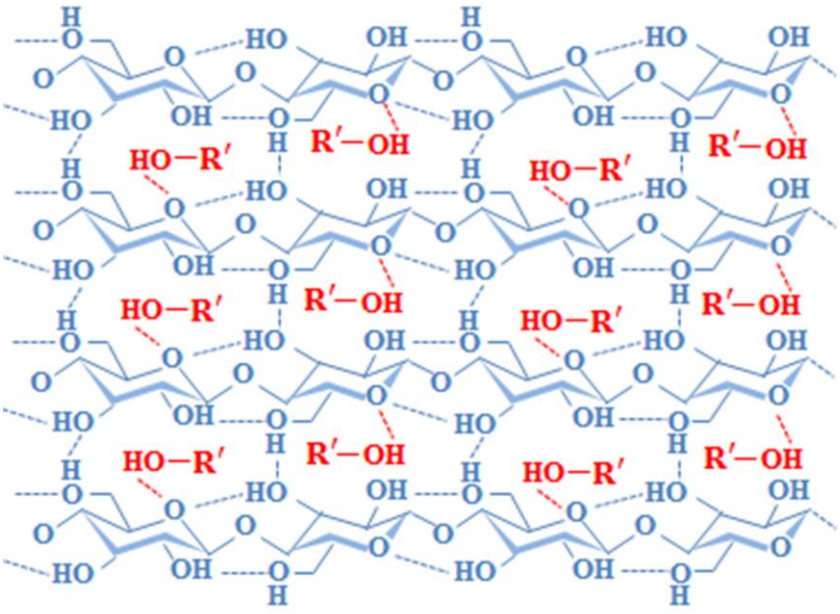

Figure S4. Schematic presentation of the structure of cellulose after the application of mechanical stress where OH-group containing elements, produced from chain breaking of PDMS make hydrogen bonding with the oxygen atom of the glucose units.[S15,S16] Reproduced with permission from reference S15. Copyright 2013 Royal Society of Chemistry.

Text S3. Piezoelectric coefficient measurment.

We have measured the piezoelectric coefficient (d_{33}) value of the hybrid composite film (which was used for fabricating HPG) using a d_{33} meter (Piezotest, PM300) under the constant applied force of 0.5 N and frequency at 49 Hz. We noticed that the value is lying between 8 to 15 pC/N, which is probably attributed to the viscoelastic behaviour of the hybrid composite film.[S17, S18] The bond breaking of PDMS under mechanical stress may also be responsible for the variation of piezoelectric coefficient (d_{33}) in between 8-15 pC/N.

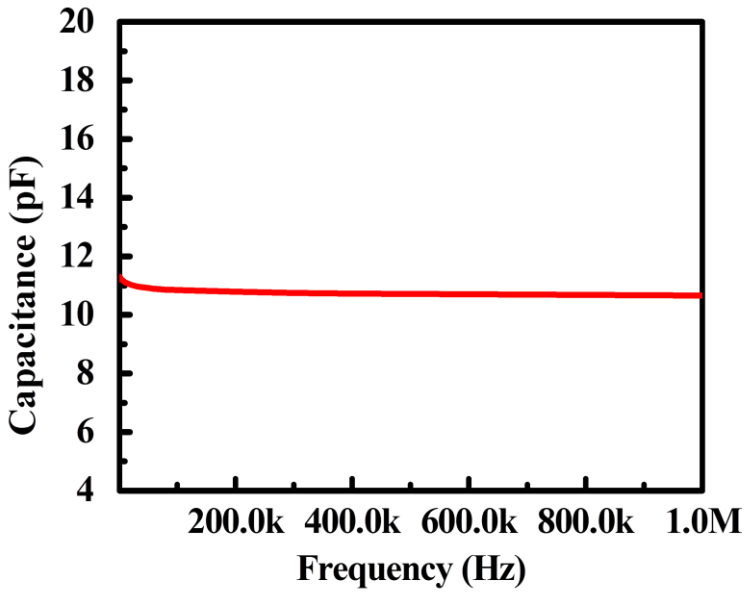

Figure S5. Capacitance versus frequency curve of the hybrid composite film, utilized for HPG fabrication.

To check the validity of the d_{33} measurement, we have performed frequency dependence capacitance (shown in Supporting Information, Figure S5**)** measurement by impedance analyser.[S19] If we use the value of capacitance and measured value of d_{33} (for example, 8 pC/N and 15 pC/N) then voltage output generated by our HGP is found to be 24 V and 45 V by using the following equation:[S20]

$$V = F \times d_{33}/C \qquad (5)$$

Where, F is applied force and C is the capacitance.

Thus, we believed that our generated output voltage is very much consistent with the piezoelectric frame of references.

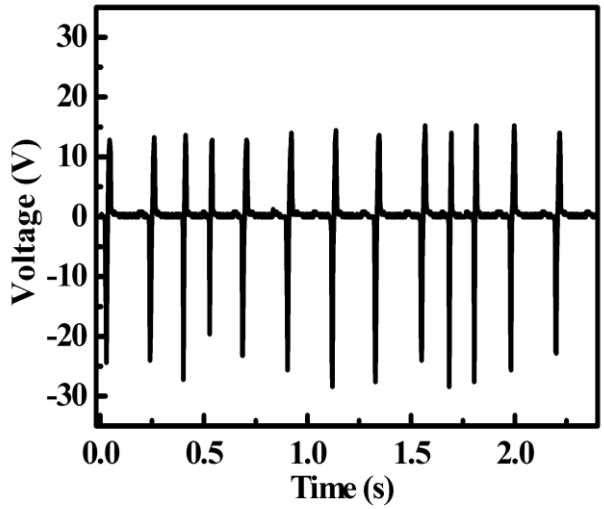

Figure S6. The open circuit voltage signals from the HPG generated in the reverse connection.

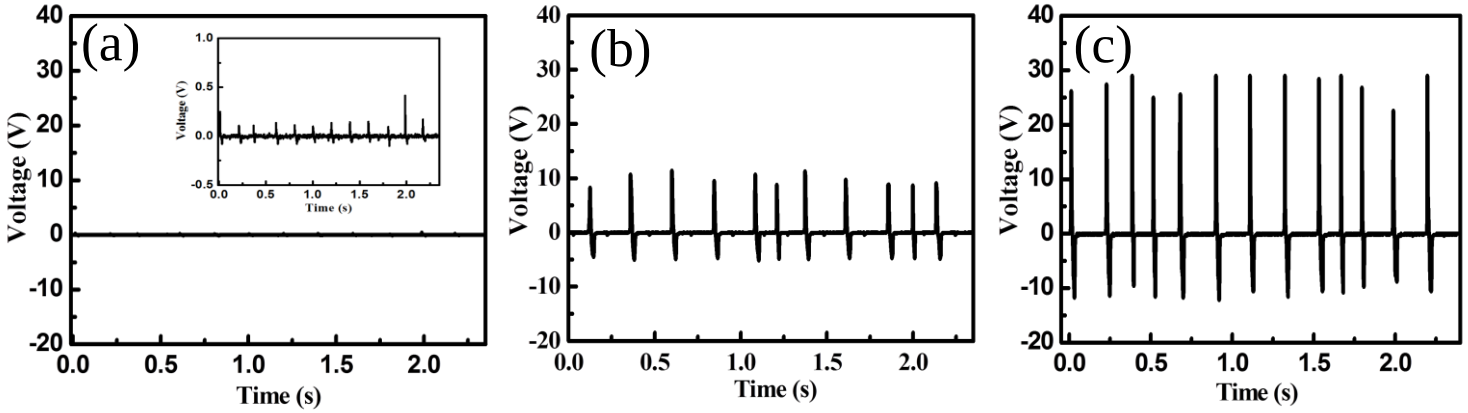

Figure S7. The open circuit voltage signals generated from HPG made with (a) PDMS-MWCNTs (inset shows the enlarge view), (b) PDMS-NCMF, (c) PDMS-NCMF-MWCNTs.

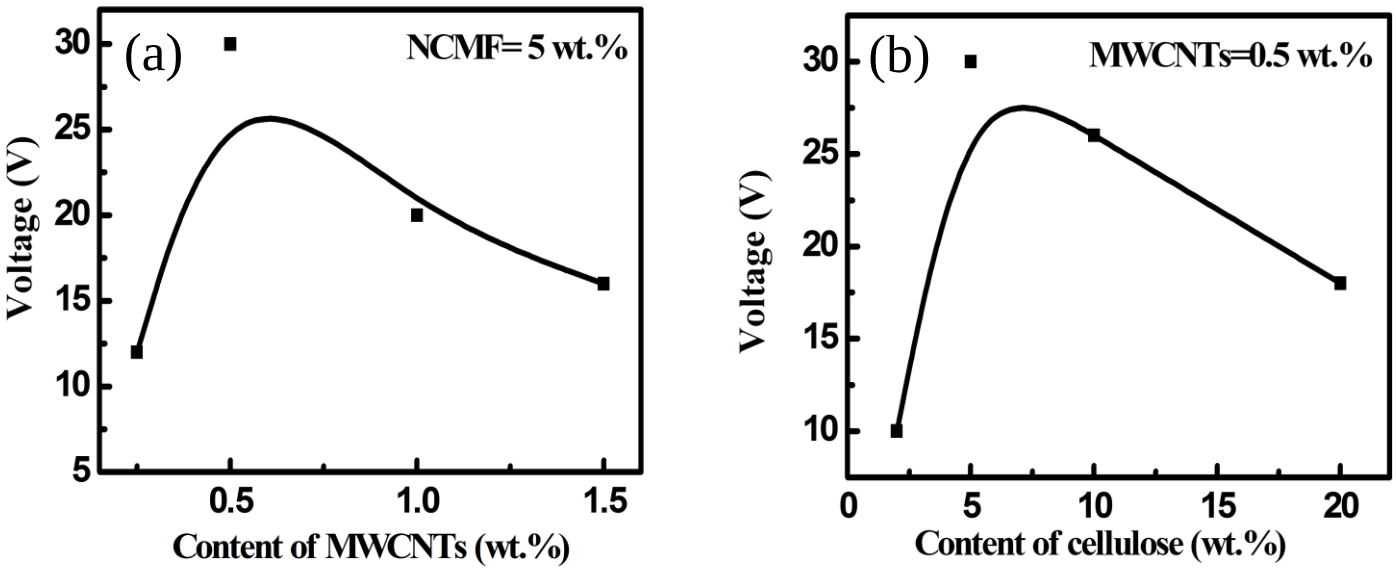

Figure S8. (a) The variation of output voltage from HPG as a function of MWCNT concentration for a fixed amount of NCMF (5 wt. %). (b) The variation of output voltage from HPG as a function of NCMF concentration for a fixed amount of MWCNTs (0.5 wt. %).

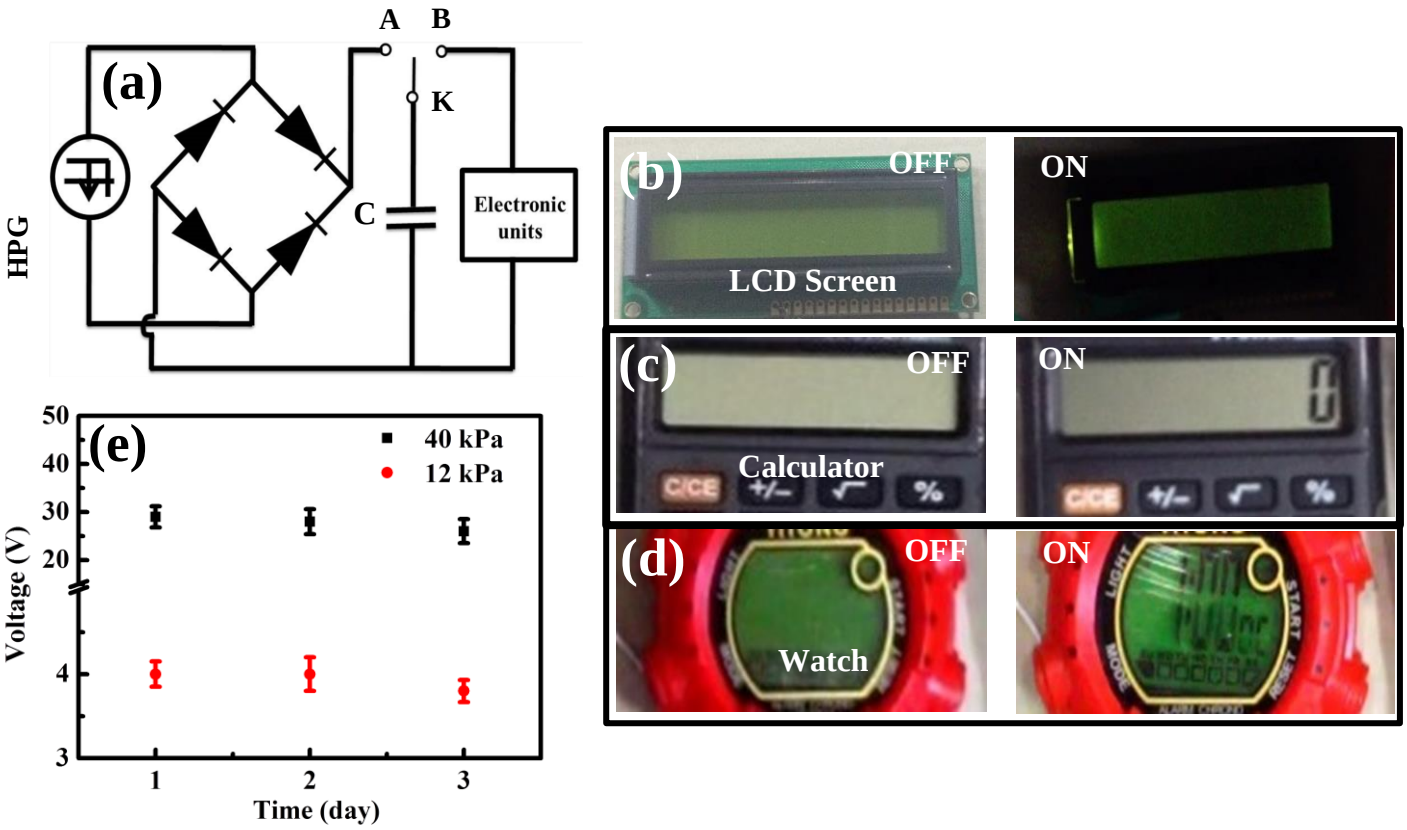

Figure S9. (a) A schematic of a circuit diagrams for capacitor charging and power up the electronic units (e.g., LCD screen, calculator and wrist watch). The AC voltage generated from the HPG is converted to DC voltage via the full wave rectifier and utilizes to charge up the capacitor (when the key "K" is connected to the point "A"). This charged capacitor then connect to an electronic unit to power up (when key "K" is connected to the point "B"). (b)−(d) Photograph of the Off and On conditions of the LCD screen, calculator and wrist watch respectively when these are powered up by charged capacitor. (e) The output voltages of the HPG under hand punching and pressure imparting probe with stress amplitude~ 40 kPa and ~12 kPa, respectively in three successive days after repeating imparting for 1500s each day (shown in Figure S10) with pressure imparting probe (Freq~7 Hz, applied pressure~12 kPa). The output voltage arises no significant change after 3 days.

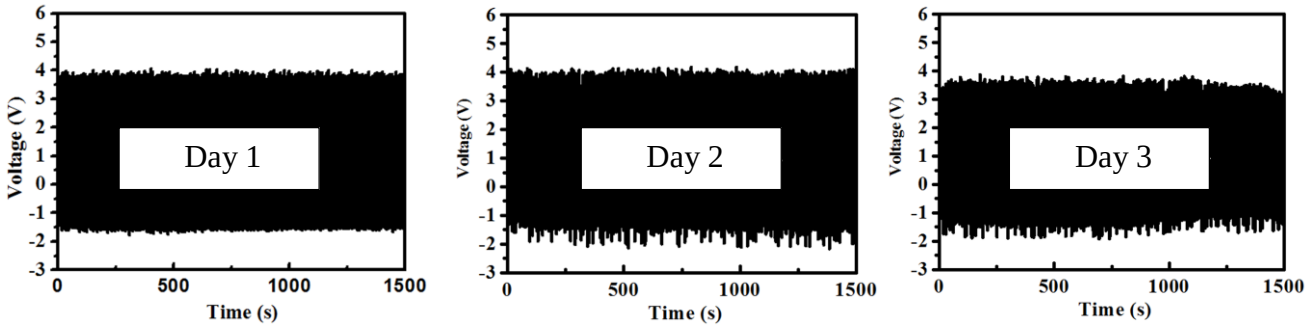

Figure S10. Stability of the HPG was tested under compressive stress amplitude of 12 kPa by pressure imparting probe (Freq~7 Hz) at different days of operation (1500 second per day).

REFERENCES

(S1) Li, J.; Qiang, D.; Zhang, M.; Xiu, H.; Zhang, X. Joint Action of Ultrasonic and Fe^{3+} to Improve Selectivity of Acid Hydrolysis for Microcrystalline Cellulose. *Carbohydr. Polym.* **2015,** *129*, 44–49.

(S2) Kamphunthong, W.; Hornsby, P.; Sirisinha K. Isolation of Cellulose Nanofibers from Para Rubberwood and their Reinforcing Effect in Poly (vinyl alcohol) Composites. *J. Appl. Polym.* **2012,** *125*, 1642−1651.

(S3) Han, J.; Zhou, C.; Wu, Y.; Liu, F.; Wu, Q. Self-Assembling Behaviour of Cellulose Nanoparticles during Freeze-Drying: Effect of Suspension Concentration, Particle Size, Crystal Structure, and Surface Charge. *Biomacromolecules* **2013**, *14*, 1529−1540.

(S4) Kavkler, K.; Demšar, A. Application of FTIR and Raman Spectroscopy to Qualitative Analysis of Structural Changes in Cellulosic Fibres. *Tekstilec* **2012**, *55*, 19–31.

(S5) Hou, C.; Huang, T.; Wang, H.; Yu, H.; Zhang, Q.; Li, Y. A Strong and Stretchable Self-Healing Film with Self-Activated Pressure Sensitivity for Potential Artificial Skin Applications. *Sci. Rep.* **2013**, DOI:10.1038/srep03138.

(S6) Alam, M. M.; Ghosh, S. K.; Sultana, A.; Mandal, D. Lead-free $ZnSnO_3$/MWCNTs-Based Self-poled Flexible Hybrid Nanogenerator for Piezoelectric Power Generation. *Nanotechnology* **2015**, *26*, 165403–165409.

(S7) Kumar, A.; Gullapalli, H.; Balakrishnan, K.; Botello-Mendez , A.; Vajtai, R.; Terrones, M. Ajayan, P. M. Flexible ZnO–Cellulose Nanocomposite for Multisource Energy Conversion. *Small* **2011**, *7,* 2173–2178.

(S8) Liao, Q.; Zhang, Z.; Zhang, X.; Mohr, M.; Zhang, Y.; Fecht, H.-J. Flexible Piezoelectric Nanogenerators Based on Fiber/ZnO Nanowires/ Paper Hybrid Structure for Energy Harvesting. *Nano Res.* **2014**, *7*, 917-930.

(S9) Lee, M.; Chen, C.-Y.; Wang, S.; Cha, S. N.; Park, Y. J.; Kim, J. M.; Chou, L.-J.; Wang, Z. L. A Hybrid Piezoelectric Structure for Wearable Nanogenerators. *Adv. Mater.* **2012**, *24*, 1759–1764.

(S10) Park, K.-I.; Lee, M.; Liu, Y.; Moon, S.; Hwang, G.-T.; Zhu, G.; Kim, J. E.; Kim, S. O.; Kim, D. K.; Wang, Z. L.; Lee, K. J. Flexible Nanocomposite Generator Made of $BaTiO_3$ Nanoparticles and Graphitic Carbons. *Adv. Mater.* **2012**, *24*, 2999–3004.

(S11) Jung, J. H.; Chen, C.-Y.; Yun, B. K.; Lee, N.; Zhou, Y.; Jo, W.; Chou, L.-J.; Wang, Z. L. Lead-free $KNbO_3$ Ferroelectric Nanorod based Flexible Nanogenerators and Capacitors. *Nanotechnology* **2012**, *23*, 375401−375407.

(S12) Joung, M.-R.; Xu, H.; Seo, I.-T.; Kim, D.-H.; Hur, J.; Nahm, S.; Kang, C.-Y.; Yoon, S.-J.; Park, H.-M. Piezoelectric Nanogenerators Synthesized using $KNbO_3$ Nanowires with Various Crystal Structures. *J. Mater. Chem. A* **2014**, *2,* 18547–18553.

(S13) Lin, Z.-H.; Yang, Y.; Wu, J. M.; Liu, Y.; Zhang, F.; Wang, Z. L. $BaTiO_3$ Nanotubes-Based Flexible and Transparent Nanogenerators. *J. Phys. Chem. Lett*. **2012**, *3*, 3599−3604.

(S14) Xue, Q.-T.; Wang, Z.; Tian, H.; Huan, Y.; Xie, Q.-Y.; Yang, Y.; Xie, D.; Li, C.; Shu, Y.; Wang, X-H.; Ren, T.-L. A Record Flexible Piezoelectric KNN Ultrafine-Grained Nanopowder-Based Nanogenerator. *AIP Adv.* **2015**, *5*, 017102−017108.

(S15) Baytekin, B.; Baytekin H. T.; Grzybowski, B. A. Retrieving and Converting Energy From Polymers: Deployable Technologies and Emerging Concepts. *Energy Environ. Sci.* **2013**, *6*, 3467–3482.

(S16) Kondo,T.; Sawatari, C.; Manley, R. S. J.; Gray, D. G. Characterization of Hydrogen Bonding in Cellulose-Synthetic Polymer Blend Systems with Regioselectively Substituted Methylcellulose. *Macromolecules* **1994,** *27*, 210-215.

(S17) Babu, I.; Meis, N.; de With, G. Measuring the Direct Piezoelectric Charge Coefficient for Polymer Matrix Composites. *Polymer Testing* **2014**, *40*, 286-289.

(S18) Sharma, S. K.; Gaur, H.; Kulkarni, M.; Patil, G.; Bhattacharya, B.; Sharma, A. PZT–PDMS Composite for Active Damping of Vibrations. *Compos. Sci. Technol.* **2013**, *77*, 42–51.

(S19) Al-Ahmad, M.; Plana, R. A Novel Method for PZT Thin Film Piezoelectric Coefficients Determination Using Conventional Impedance Analyzer, Proce. 37th European Microwave Conf., Oct., **2007**, Germany.

(S20) Mahadeva, S. K.; Walus, K.; Stoeber, B. Piezoelectric Paper Fabricated via Nanostructured Barium Titanate Functionalization of Wood Cellulose Fibers. *ACS Appl. Mater. Interfaces* **2014**, *6*, 7547−7553.

Video 1- Power up the LED

Video 2- Power up the LCD screen